

MINKOWSKI PLANE, CONFOCAL CONICS, AND BILLIARDS

Vladimir Dragović and Milena Radnović

ABSTRACT. Geometry of confocal conics in the Minkowski plane and related billiard dynamics are studied in details. Periodic trajectories are described and several new examples are presented. Topological properties of the elliptical billiards are analyzed and the results are formulated in the terms of the Fomenko graphs.

1. Introduction

Geometry of confocal families of quadrics in pseudo-Euclidean spaces of arbitrary dimension d and any signature, and related billiard dynamics have recently been studied by the authors in [8]. With a goal to give a complete description of periodic billiard trajectories within ellipsoids, there we introduced a new discrete combinatorial-geometric structure associated to a confocal pencil of quadrics, by which the quadrics were decomposed into new relativistic quadrics.

The aim of the present paper is, staying focused to the two-dimensional case, to explain in more detail constructions from [8] and to provide new results and examples.

In Section 2 we list necessary introductory notions and definitions for the Minkowski plane, together with definition and properties of confocal families and relativistic conics.

In Section 3, we consider elliptical billiards. In Section 3.2, we derive analytic Cayley-type conditions for periodic trajectories of elliptical billiard in the Minkowski plane. Such conditions, for ellipsoidal billiards in the pseudo-Euclidean

2010 *Mathematics Subject Classification*: 37J3, 70H06, 70H12.

Key words and phrases: Confocal conics, Poncelet theorem, periodic billiard trajectories, Minkowski plane, light-like billiard trajectories.

The research which led to this paper was partially supported by the Serbian Ministry of Education and Science (Project no. 174020: *Geometry and Topology of Manifolds and Integrable Dynamical Systems*) and by Mathematical Physics Group of the University of Lisbon (Project *Probabilistic approach to finite and infinite dimensional dynamical systems*, PTDC/MAT/104173/2008). M. R. is grateful to the Weizmann Institute of Science (Rehovot, Israel) and *The Abdus Salam* ICTP (Trieste, Italy) for their hospitality and support in various stages of work on this paper.

spaces of the arbitrary dimensions, are derived in [8]. Here we give another proof, adopted to the planar case, see Theorem 3.1. In the next Section 3.3, we study light-like trajectories of such billiards and derive a periodicity criterion in a simple form, see Theorem 3.2. That criterion, from [8], is proved here in the algebro-geometric way. The equivalence of this simple criterion with the more complicated condition of Cayley's type is illustrated by several new examples. The equivalence of the elliptical billiard flow to a certain rectangular billiard flow is stated in Theorem 3.3, while for the proof we refer the reader to [8]. In Section 3.4, we conclude with a complete description of topological properties of elliptical billiards in the Minkowski plane. We are using Fomenko invariants, see Theorem 3.4, as we did in the Euclidean case in [6, 7]. The results from Section 3.4 are new.

2. Confocal conics in the Minkowski plane

We start by giving necessary notions of the Minkowski plane in Section 2.1 and we review properties of confocal families of conics in the Minkowski plane in Section 2.2. In Section 2.3, relativistic conics are presented, following [1], see also [8].

2.1. The Minkowski plane. *The Minkowski plane is \mathbf{R}^2 with the Minkowski scalar product*

$$(2.1) \quad \langle x, y \rangle = x_1 y_1 - x_2 y_2.$$

The Minkowski distance between points x, y is $\text{dist}(x, y) = \sqrt{\langle x - y, x - y \rangle}$. Since the scalar product can be negative, notice that the Minkowski distance can have imaginary values as well. In that case, we choose the value of the square root with the positive imaginary part.

Let ℓ be a line in the Minkowski plane, and v its vector. ℓ is called:

- *space-like* if $\langle v, v \rangle > 0$;
- *time-like* if $\langle v, v \rangle < 0$;
- and *light-like* if $\langle v, v \rangle = 0$.

Two vectors x, y are *orthogonal* in the Minkowski plane if $\langle x, y \rangle = 0$. Note that a light-like vector is orthogonal to itself.

2.2. Confocal families of conics. Here, we give a review of basic properties of families of confocal conics in the Minkowski plane, see [8].

Denote by

$$(2.2) \quad \mathcal{E} : \frac{x^2}{a} + \frac{y^2}{b} = 1$$

an ellipse in the plane, with a, b being fixed positive numbers.

The associated family of confocal conics is

$$(2.3) \quad \mathcal{C}_\lambda : \frac{x^2}{a - \lambda} + \frac{y^2}{b + \lambda} = 1, \quad \lambda \in \mathbf{R}.$$

The family is shown in Figure 1. We may distinguish the following three sub-families in the family (2.3):

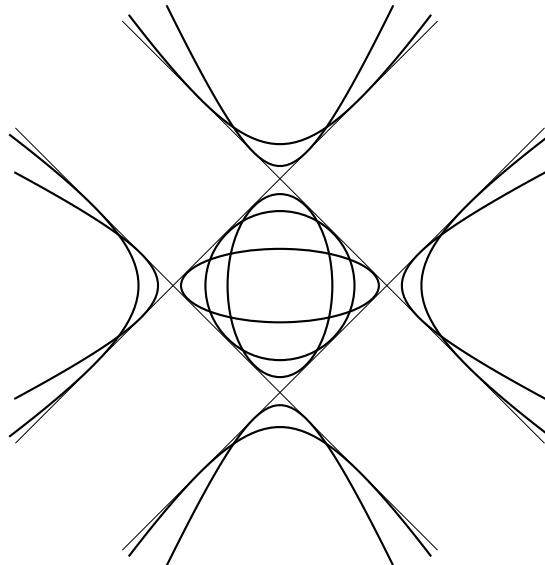


FIGURE 1. Family of confocal conics in the Minkowski plane.

- for $\lambda \in (-b, a)$, conic \mathcal{C}_λ is an ellipse;
- for $\lambda < -b$, conic \mathcal{C}_λ is a hyperbola with x -axis as the major one;
- for $\lambda > a$, it is a hyperbola again, but now its major axis is y -axis.

In addition, there are three degenerated quadrics: $\mathcal{C}_a, \mathcal{C}_{-b}, \mathcal{C}_\infty$, corresponding to y -axis, x -axis, and the line at the infinity respectively. The confocal family has three pairs of foci: $F_1(\sqrt{a+b}, 0), F_2(-\sqrt{a+b}, 0)$; $G_1(0, \sqrt{a+b}), G_2(0, -\sqrt{a+b})$; and $H_1(1 : -1 : 0), H_2(1 : 1 : 0)$ on the line at the infinity.

We notice four distinguished lines:

$$\begin{aligned} x + y &= \sqrt{a+b}, & x + y &= -\sqrt{a+b}, \\ x - y &= \sqrt{a+b}, & x - y &= -\sqrt{a+b}. \end{aligned}$$

These lines are common tangents to all conics from the family.

Conics in the Minkowski plane have geometric properties analogous to the conics in the Euclidean plane. Namely, for each point on conic \mathcal{C}_λ , either sum or difference of its Minkowski distances from the foci F_1 and F_2 is equal to $2\sqrt{a-\lambda}$; either sum or difference of the distances from the other pair of foci G_1, G_2 is equal to $2\sqrt{-b-\lambda}$ [8].

2.3. Relativistic conics. In the Minkowski plane, it is natural to consider relativistic conics, which are suggested in [1]. In this subsection, we give a brief account of the related analysis.

Consider points $F_1(\sqrt{a+b}, 0)$ and $F_2(-\sqrt{a+b}, 0)$.

For a given constant $c \in \mathbf{R}^+ \cup i\mathbf{R}^+$, a *relativistic ellipse* is the set of points X satisfying $\text{dist}(F_1, X) + \text{dist}(F_2, X) = 2c$, while a *relativistic hyperbola* is the union of the sets given by the following equations:

$$\begin{aligned} \text{dist}(F_1, X) - \text{dist}(F_2, X) &= 2c, \\ \text{dist}(F_2, X) - \text{dist}(F_1, X) &= 2c. \end{aligned}$$

Relativistic conics can be described as follows.

- $0 < c < \sqrt{a+b}$: The corresponding relativistic conics lie on ellipse \mathcal{C}_{a-c^2} from family (2.3). The ellipse \mathcal{C}_{a-c^2} is split into four arcs by touching points with the four common tangent lines; thus, the relativistic ellipse is the union of the two arcs intersecting the y -axis, while the relativistic hyperbola is the union of the other two arcs.
- $c > \sqrt{a+b}$: The relativistic conics lie on \mathcal{C}_{a-c^2} —a hyperbola with x -axis as the major one. Each branch of the hyperbola is split into three arcs by touching points with the common tangents; thus, the relativistic ellipse is the union of the two finite arcs, while the relativistic hyperbola is the union of the four infinite ones.
- c is **imaginary**: The relativistic conics lie on hyperbola \mathcal{C}_{a-c^2} —a hyperbola with y -axis as the major one. As in the previous case, the branches are split into six arcs in total by common points with the four tangents. The relativistic ellipse is the union of the four infinite arcs, while the relativistic hyperbola is the union of the two finite ones.

The conics are shown in Figure 2.

Notice that all relativistic ellipses are disjoint one with another, as well as all relativistic hyperbolas. Moreover, at the intersection point of a relativistic ellipse which is a part of the geometric conic \mathcal{C}_{λ_1} from the confocal family (2.3) and a relativistic hyperbola belonging to \mathcal{C}_{λ_2} , it is always $\lambda_1 < \lambda_2$.

3. Elliptical billiards

Elliptical billiards in Euclidean plane have been studied intensively, see for example [13] and [7] and references therein. These billiards serve as a paradigm of complete integrable discrete systems. They can be seen as discretizations of geodesics on ellipsoids as well. In the setting of Minkowski geometry, geodesics on ellipsoidis have been studied recently in [9]. Related billiard systems in pseudo-Euclidean geometry were studied in [12], and then in [8]. Such billiard systems are closely related to a recent concept of contact complete integrability, introduced in [11], see also [10].

3.1. Billiard reflection in the Minkowski plane. Let v be a vector and p a line in the Minkowski plane. Decompose vector v into the sum $v = a + n_p$ of a vector n_p orthogonal to p and a belonging to p . Then vector $v' = a - n_p$ is the *billiard reflection* of v on p . It is easy to see that v is also the billiard reflection of v' with respect to p . Moreover, since $\langle v, v \rangle = \langle v', v' \rangle$, vectors v, v' are of the same type.

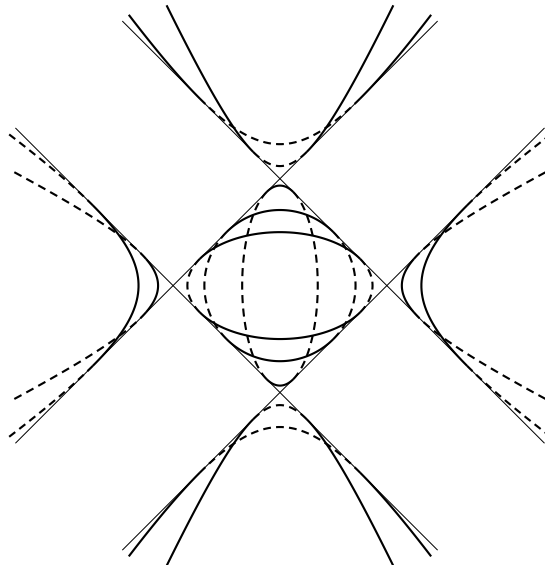


FIGURE 2. Relativistic conics in the Minkowski plane: relativistic ellipses are represented by full lines, and hyperbolas by dashed ones.

Note that $v = v'$ if v is contained in p and $v' = -v$ if it is orthogonal to p . If n_p is light-like, which means that it belongs to p , then the reflection is not defined.

Line ℓ' is *the billiard reflection* of ℓ off a smooth curve \mathcal{S} if their intersection point $\ell \cap \ell'$ belongs to \mathcal{S} and the vectors of ℓ, ℓ' are reflections of each other with respect to the tangent line of \mathcal{S} at this point.

The lines containing segments of a given billiard trajectory within \mathcal{S} are all of the same type: they are all either space-like, time-like, or light-like.

Now, take \mathcal{S} to be ellipse \mathcal{E} . Then it is possible to extend the reflection mapping to those points where the tangent lines contain the orthogonal vectors. Namely, the limit of the motion in the neighborhood of such points is that the billiard particle, after collision with the boundary, would move exactly in the opposite direction. Thus, at such points, we define that a vector reflects into the opposite one, i.e. $v' = -v$ and $\ell' = \ell$. Since close trajectories reflect two times in the neighborhood, it is natural to count each such reflection twice. For the detailed explanation, see [12].

Billiard trajectories within ellipses in the Minkowski plane have caustic properties: each segment of a given trajectory will be tangent to the same conic confocal with the boundary, see [8].

The famous focal property also holds: if one line containing the initial segment of a given trajectory within an ellipse of the family (2.3) contains a focus of the family, say F_1, G_1 , or H_1 , then the line containing the next segment will pass

through F_2 , G_2 , or H_2 respectively, unless the tangent line to the boundary at the reflection point is light-like.

3.2. Periodic trajectories of elliptical billiard. Analytic conditions for existence of closed polygonal lines inscribed in one conic and circumscribed about another one in the projective plane are derived by Cayley [3,4]. They can be applied to billiard trajectories within ellipses in the Minkowski plane as well, since each such trajectory has a caustic among confocal conics. In this section, we shall analyze in more detail some particular properties related to the Minkowski geometry.

THEOREM 3.1. *In the Minkowski plane, consider a billiard trajectory \mathcal{T} within ellipse \mathcal{E} given by equation (2.2).*

The trajectory is periodic with period $n = 2m$ if and only if the following condition is satisfied:

$$(3.1) \quad \det \begin{pmatrix} B_3 & B_4 & \dots & B_{m+1} \\ B_4 & B_5 & \dots & B_{m+2} \\ \dots & \dots & \dots & \dots \\ B_{m+1} & B_{m+2} & \dots & B_{2m-1} \end{pmatrix} = 0.$$

Trajectory \mathcal{T} is periodic with period $n = 2m + 1$ if and only if \mathcal{C}_α is an ellipse and the following condition is satisfied:

$$(3.2) \quad \det \begin{pmatrix} B_3 & B_4 & \dots & B_{m+2} \\ \dots & \dots & \dots & \dots \\ B_{m+1} & B_{m+2} & \dots & B_{2m} \\ C_{m+1} & C_{m+2} & \dots & C_{2m} \end{pmatrix} = 0.$$

Here:

$$\begin{aligned} \sqrt{(a-t)(b+t)(\alpha-t)} &= B_0 + B_1 t + B_2 t^2 + \dots, \\ \sqrt{\frac{(a-t)(b+t)}{\alpha-t}} &= C_0 + C_1 t + C_2 t^2 + \dots \end{aligned}$$

are the Taylor expansions around $t = 0$.

PROOF. Each point inside \mathcal{E} is the intersection of exactly two ellipses \mathcal{C}_{λ_1} and \mathcal{C}_{λ_2} from (2.3). Parameters λ_1, λ_2 are generalized Jacobi coordinates. Take $\lambda_1 < \lambda_2$.

Consider first the case when \mathcal{C}_α is a hyperbola. Then along \mathcal{T} these coordinates will take values in segments $[-b, 0]$ and $[0, a]$ respectively with the endpoints of the segments as the only local extrema. λ_1 achieves value $-b$ at the intersections of \mathcal{T} with the x -axis, while λ_2 achieves a at the intersections with y -axis. At each reflection point, one of the coordinates achieves value 0. They can both be equal to 0 only at the points where \mathcal{E} has a light-like tangent, and there reflection is counted twice.

This means that on a closed trajectory the number of reflections is equal to the number of intersection points with the coordinate axes. Since a periodic trajectory crosses each of the coordinate axes even number of times, the first part of the theorem is proved.

The condition on \mathcal{T} to become closed after n reflections on \mathcal{E} , n_1 crossings over x -axis, and n_2 over y -axis is that the equality $n_1P_a + n_2P_{-b} = nP_0$ holds on the elliptic curve $s^2 = (a-t)(b+t)(\alpha-t)$, where by P_β we denoted a point on the curve corresponding to $t = \beta$, and P_∞ is taken to be the neutral for the elliptic curve group.

From the previous discussion, $n_1 + n_2 = n$ and all three numbers are even. P_a and P_{-b} are branching points of the curve, thus $2P_a = 2P_{-b} = 2P_\infty$, so the condition becomes $nP_0 = nP_\infty$, which is equivalent to (3.1).

Now suppose \mathcal{C}_α is an ellipse. The generalized Jacobi coordinates take values in segments $[-b, 0]$, $[0, \alpha]$ or in $[\alpha, 0]$, $[0, a]$, depending on the sign of α . Since both cases are processed in a similar way, we assume $\alpha < 0$.

Coordinate λ_1 has extrema on \mathcal{T} at the touching points with the caustic and some of the reflection points, while λ_2 has extrema at the crossing points with y -axis and some of the reflection points.

The condition on \mathcal{T} to become closed after n reflections on \mathcal{E} , with n_1 crossings over y -axis, and n_2 touching points with the caustic is $n_1P_a + n_2P_\alpha = nP_0$, with $n_1 + n_2 = n$ and n_1 even.

Thus, for n even we get (3.1) in the same manner as for a hyperbola as a caustic.

For n odd, the condition is equivalent to $nP_0 = (n-1)P_\infty + P_\alpha$. Notice that one basis of the space $\mathcal{L}((n-1)P_\infty + P_\alpha)$ is

$$1, t, \dots, t^m, s, ts, \dots, t^{m-2}s, \frac{s}{t-\alpha}.$$

Using this basis, as it is shown in [5, 7], we obtain (3.2). \square

EXAMPLE 3.1 (3-periodic trajectories). Let us find all 3-periodic trajectories within ellipse \mathcal{E} given by (2.2) in the Minkowski plane, i.e., all conics \mathcal{C}_α from the confocal family (2.3) corresponding to such trajectories.

The condition is

$$C_2 = \frac{3a^2b^2 + 2a^2b\alpha - 2ab^2\alpha - a^2\alpha^2 - 2ab\alpha^2 - b^2\alpha^2}{8(ab)^{3/2}\alpha^{5/2}} = 0,$$

which gives the following solutions for the parameter α of the caustic:

$$\alpha_1 = \frac{ab}{(a+b)^2} (a-b-2\sqrt{a^2+ab+b^2}),$$

$$\alpha_2 = \frac{ab}{(a+b)^2} (a-b+2\sqrt{a^2+ab+b^2}).$$

Notice that $-b < \alpha_1 < 0 < \alpha_2 < a$ so both caustics \mathcal{C}_{α_1} , \mathcal{C}_{α_2} are ellipses.

EXAMPLE 3.2 (4-periodic trajectories). By Theorem 3.1, the condition is $B_3 = 0$. Since

$$B_3 = \frac{(-ab - a\alpha + b\alpha)(-ab + a\alpha + b\alpha)(ab + a\alpha + b\alpha)}{16(ab\alpha)^{5/2}},$$

we obtain the following solutions:

$$\alpha_1 = \frac{ab}{b-a}, \quad \alpha_2 = \frac{ab}{a+b}, \quad \alpha_3 = -\frac{ab}{a+b}.$$

Since $\alpha_1 \notin (-b, a)$ and $\alpha_2, \alpha_3 \in (-b, a)$, conic \mathcal{C}_{α_1} is a hyperbola, while $\mathcal{C}_{\alpha_2}, \mathcal{C}_{\alpha_3}$ are ellipses.

EXAMPLE 3.3 (5-periodic trajectories). The condition is

$$\det \begin{pmatrix} B_3 & B_4 \\ C_3 & C_4 \end{pmatrix} = 0.$$

Taking $a = b = 1$, we get that this is equivalent to $64\alpha^6 - 16\alpha^4 - 52\alpha^2 + 5 = 0$. This equation has four solutions in \mathbf{R} , all four contained in $(-1, 1)$, and two conjugated solutions in \mathbf{C} .

REMARK 3.1. For the analytic description of the periodic billiard trajectories within ellipsoids in the higher-dimensional pseudo-Euclidean spaces, see [8]. For the Euclidean case, see [7] and references therein. Some aspects have recently been discussed in [14].

3.3. Light-like trajectories. In this section we consider in more detail light-like trajectories of elliptical billiard, see Figure 3 for an example of such a trajectory. We are going to review results from [8] and illustrate them by some examples.

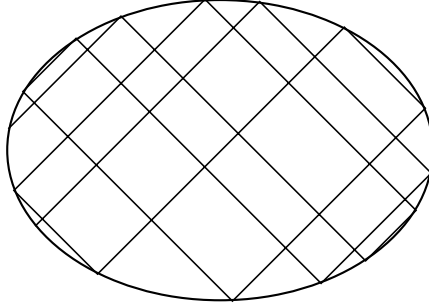


FIGURE 3. Light-like billiard trajectory.

Periodic light-like trajectories. Let us first notice that segments of light-like billiard trajectories are alternately parallel to two light-like directions in the plane (see Figure 3), thus a trajectory can close only after even number of reflections.

The analytic condition for n -periodicity of light-like billiard trajectory within the ellipse \mathcal{E} given by equation (2.2) can be derived as in Theorem 3.1. We get the condition stated in (3.1), with $\alpha = \infty$, i.e., (B_i) are coefficients in the Taylor expansion around $t = 0$ of $\sqrt{(a-t)(b+t)} = B_0 + B_1t + B_2t^2 + \dots$.

Now, we are going to derive analytic condition for periodic light-like trajectories in another way, which will lead to a more compact form of (3.1).

THEOREM 3.2. *Light-like billiard trajectory within ellipse \mathcal{E} is periodic with period n , where n is an even integer if and only if*

$$(3.3) \quad \arctan \sqrt{a/b} \in \left\{ \frac{k\pi}{n} \mid 1 \leq k < \frac{n}{2}, \left(k, \frac{n}{2}\right) = 1 \right\}.$$

PROOF. The isospectral curve for elliptic billiard with caustic \mathcal{C}_∞ is the rational curve $y^2 = (x-a)(x+b)$, with the two infinite points identified. Condition for n -periodicity of a light-like trajectory is that divisors nP_0 and nP_{-b} are equivalent on this curve with one singular point. Here, P_0 is one of the points corresponding to the value $x = 0$, P_{-b} corresponds to $x = -b$, $y = 0$. Denote by P_∞^+ , P_∞^- the points at infinity corresponding to lines $x = y$ and $x = -y$ respectively. On the isospectral curve, P_∞^+ and P_∞^- are identified.

Introduce the following reparametrization of the curve: $t = \frac{y}{x+b} = \left(\frac{x-a}{x+b}\right)^{1/2}$. Then $t(P_0) = i\sqrt{a/b}$, $t(P_{-b}) = \infty$, $t(P_\infty^+) = 1$, $t(P_\infty^-) = -1$. Up to a constant factor, there is a unique rational function with the only zero of order n at P_0 and a pole of order n at P_{-b} :

$$f = (t - i\sqrt{a/b})^n t^{-n}.$$

We need to check if f has the same values at P_∞^+ and P_∞^- , i.e., $(1 - i\sqrt{a/b})^n = (-1 - i\sqrt{a/b})^n$. Since n is even, this can be true only if $(1 - i\sqrt{a/b})^n$ is real. Thus, (3.3) follows. \square

REMARK 3.2. A simpler and more elementary proof of Theorem 3.2 is given in [8]. The one presented here is interesting and instructive because of the algebro-geometric tools involved.

As an immediate consequence, we get

COROLLARY 3.1. *For a given even integer n , the number of different ratios of the axes of ellipses having n -periodic light-like billiard trajectories is equal to:*

$$\begin{cases} \varphi(n)/2, & \text{if } n \text{ is not divisible by } 4, \\ \varphi(n)/4, & \text{if } n \text{ is divisible by } 4. \end{cases}$$

φ is Euler's totient function, i.e., the number of positive integers not exceeding n that are relatively prime to n .

REMARK 3.3. There are four points on \mathcal{E} where the tangents are light-like. Those points cut four arcs on \mathcal{E} . An n -periodic trajectory within \mathcal{E} hits each one of a pair of opposite arcs exactly k times, and $\frac{n}{2} - k$ times the arcs from the other pair.

EXAMPLE 3.4 (4-periodic light-like trajectories). It is elementary to see that only circles allow such a trajectory. However, we can also deduce it from condition (3.1). For $n = 4$, this condition reads $B_3 = 0$ with $B_3 = \frac{(a-b)(a+b)^2}{16(ab)^{5/2}}$. Thus, it is equivalent to $a = b$.

On the other hand, condition (3.3) states $\sqrt{a/b} = \tan \frac{\pi}{4} = 1$.

EXAMPLE 3.5 (6-periodic light-like trajectory). For $n = 6$, the condition (3.1) is

$$\det \begin{pmatrix} B_3 & B_4 \\ B_4 & B_5 \end{pmatrix} = 0,$$

which is equivalent to

$$\frac{(a - 3b)(3a - b)(a + b)^6}{(4ab)^7} = 0.$$

Thus, we get that light-like billiard trajectories are 6-periodic in ellipses with the ratio of the axes equal to $\sqrt{3}$.

From condition (3.3), we get the same:

$$\sqrt{\frac{a}{b}} \in \left\{ \tan \frac{\pi}{6}, \tan \frac{\pi}{3} \right\} = \left\{ \sqrt{3}, \frac{1}{\sqrt{3}} \right\}.$$

A few 6-periodic trajectories are shown in Figure 4.

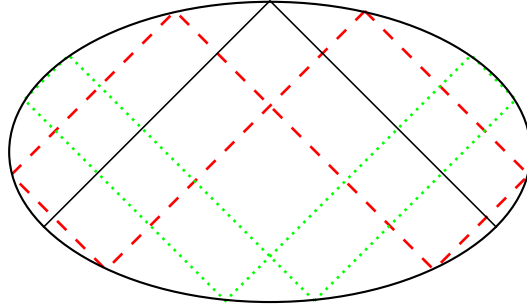


FIGURE 4. Light-like billiard trajectories with period 6 in the ellipse satisfying $a = 3b$.

EXAMPLE 3.6 (8-periodic light-like trajectories). For $n = 8$, the condition (3.1) is

$$\det \begin{pmatrix} B_3 & B_4 & B_5 \\ B_4 & B_5 & B_6 \\ B_5 & B_6 & B_7 \end{pmatrix} = \frac{(a - b)(a + b)^{12}(a^2 - 6ab + b^2)}{2^{25}(ab)^{13} \cdot \sqrt{ab}} = 0.$$

From here, we get that light-like billiard trajectories are 8-periodic in ellipses with the ratio of the axes equal to $1 + \sqrt{2}$.

Condition (3.3) gives:

$$\sqrt{\frac{a}{b}} \in \left\{ \tan \frac{\pi}{8}, \tan \frac{3\pi}{8} \right\} = \{ \sqrt{2} - 1, \sqrt{2} + 1 \}.$$

A few of such trajectories are shown in Figure 5.

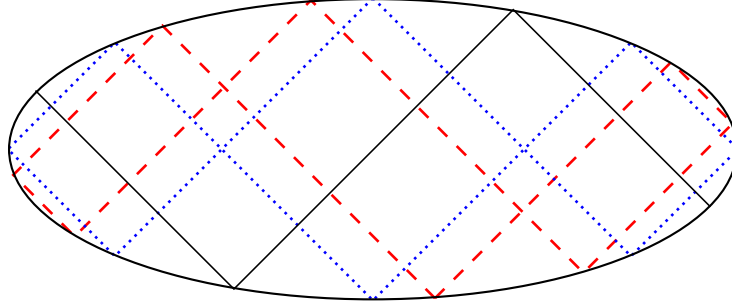


FIGURE 5. Light-like billiard trajectories with period 8 in the ellipse satisfying $a = (3 + 2\sqrt{2})b$.

EXAMPLE 3.7 (10-periodic light-like trajectories). For $n = 10$, the condition (3.1) is

$$\det \begin{pmatrix} B_3 & B_4 & B_5 & B_6 \\ B_4 & B_5 & B_6 & B_7 \\ B_5 & B_6 & B_7 & B_8 \\ B_6 & B_7 & B_8 & B_9 \end{pmatrix} = \frac{(a+b)^{20}(5a^2 - 10ab + b^2)(a^2 - 10ab + 5b^2)}{(4ab)^{22}} = 0.$$

From here, we get that light-like billiard trajectories are 10-periodic in ellipses with the ratio of the axes equal to either $\sqrt{1 + 2/\sqrt{5}}$ or $\sqrt{5 + 2\sqrt{5}}$.

From condition (3.3), we get

$$\sqrt{\frac{a}{b}} \in \left\{ \tan \frac{\pi}{10}, \tan \frac{2\pi}{10}, \tan \frac{3\pi}{10}, \tan \frac{4\pi}{10} \right\}.$$

Since

$$\begin{aligned} \tan \frac{\pi}{10} &= \sqrt{1 - 2/\sqrt{5}} = \frac{1}{\sqrt{5 + 2\sqrt{5}}} = \frac{1}{\tan \frac{4\pi}{10}} \\ \tan \frac{3\pi}{10} &= \sqrt{1 + 2/\sqrt{5}} = \frac{1}{\sqrt{5 - 2\sqrt{5}}} = \frac{1}{\tan \frac{2\pi}{10}}, \end{aligned}$$

both conditions give the same result.

A few of such trajectories are shown in Figures 6 and 7.

EXAMPLE 3.8 (12-periodic light-like trajectories). For $n = 12$, the condition (3.1) is

$$\det \begin{pmatrix} B_3 & B_4 & B_5 & B_6 & B_7 \\ B_4 & B_5 & B_6 & B_7 & B_8 \\ B_5 & B_6 & B_7 & B_8 & B_9 \\ B_6 & B_7 & B_8 & B_9 & B_{10} \\ B_7 & B_8 & B_9 & B_{10} & B_{11} \end{pmatrix} = 0,$$

which can be transformed into

$$\frac{(a-3b)(a-b)(3a-b)(a+b)^{30}(a^2-14ab+b^2)}{(4ab)^{22}\sqrt{ab}} = 0.$$

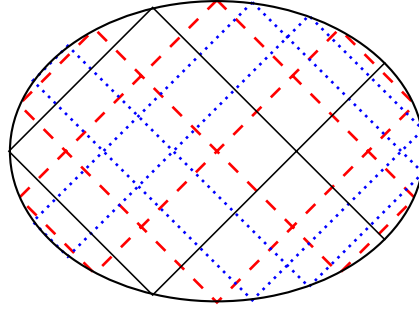


FIGURE 6. Light-like billiard trajectories with period 10 in the ellipse satisfying $a = (1 + 2/\sqrt{5})b$.

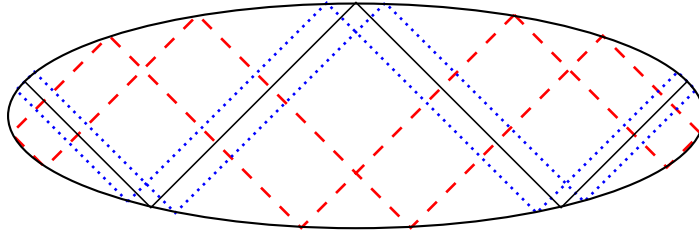


FIGURE 7. Light-like billiard trajectories with period 10 in the ellipse satisfying $a = (5 + 2\sqrt{5})b$.

From here, we get that light-like billiard trajectories are 12-periodic in ellipses with the ratio of the axes equal to $2 + \sqrt{3}$.

On the other hand, condition (3.3) gives

$$\sqrt{\frac{a}{b}} \in \left\{ \tan \frac{\pi}{12}, \tan \frac{5\pi}{12} \right\} = \{2 - \sqrt{3}, 2 + \sqrt{3}\}.$$

A few of such trajectories, obtained by a computer simulation, are shown in Figure 8.

Light-like trajectories in ellipses and rectangular billiards.

THEOREM 3.3. *The flow of light-like billiard trajectories within ellipse \mathcal{E} is trajectoryally equivalent to the flow of those billiard trajectories within a rectangle whose angle with the sides is $\frac{\pi}{4}$. The ratio of the sides of the rectangle is equal to*

$$\frac{\pi}{2 \arctan \sqrt{a/b}} - 1.$$

REMARK 3.4. The flow of light-like billiard trajectories within a given oval in the Minkowski plane will be trajectoryally equivalent to the flow of certain trajectories within a rectangle whenever invariant measure m on the oval exists such that

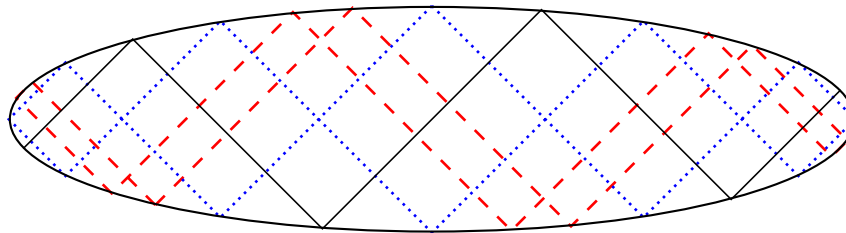


FIGURE 8. Light-like billiard trajectories with period 12 in the ellipse satisfying $a = (7 + 4\sqrt{3})b$.

$m(AB) = m(CD)$ and $m(BC) = m(AD)$, where A, B, C, D are points on the oval where the tangents are light-like.

3.4. Topological properties of elliptical billiards. Here, we are going to present the topological description of elliptical billiard in the Minkowski plane. In order to do this, we use Fomenko invariants, see [2] and references therein. The corresponding analysis for the Euclidean case has been done in [6].¹

THEOREM 3.4. *The isoenergy manifold corresponding to the billiard system within ellipse \mathcal{E} (2.2) in the Minkowski plane is represented by the Fomenko graph in Figure 9.*

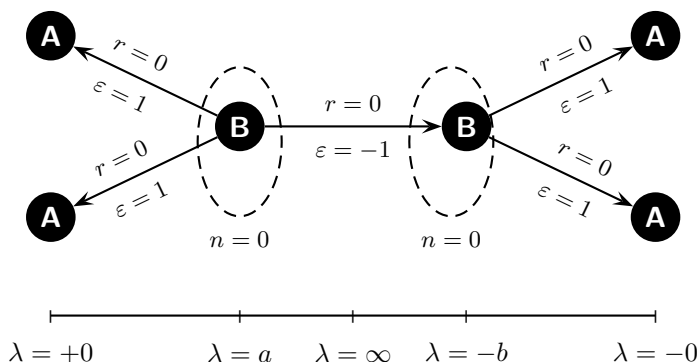


FIGURE 9. Fomenko graph for elliptical billiard in the Minkowski plane.

¹The authors are thankful to Victoria Fokicheva and Dmitry Tonkonog for their useful remark on the Fomenko graph for elliptical billiard in the Euclidean plane.

PROOF. Each level set of the isoenergy manifold corresponds to the billiard motion with a fixed caustic \mathcal{C}_λ , $\lambda \in \mathbf{R} \cup \{\infty\}$.

For $\lambda \notin \{0, a, -b\}$, the level sets are non-degenerate. The level set is a torus when the caustic is a hyperbola, i.e., for $\lambda \in (a, +\infty) \cup (-\infty, -b) \cup \{\infty\}$. If $\lambda \in (0, a) \cup (-b, 0)$ the caustic is an ellipse, and the level set is a union of two tori.

If $\lambda = -b$, the level set contains one periodic trajectory which is placed along y -axis and homoclinic trajectories, which are naturally grouped onto two separatrices—each one being projected onto the other side of the y -axis. The same, just with respect to the x -axis, holds for the level set corresponding to $\lambda = a$. Those level sets are represented by Fomenko atom **B**.

Let us consider the limit case $\lambda = 0$, when the caustic coincides with the billiard table edge. In this case, the limit motion will take place on the four arcs on the \mathcal{E} whose ends are touching points with four joint tangents of the confocal family (2.3). More precisely, if λ approaches zero from below, then the limit motion will take place on the two arcs on the left and on the right side of y -axis; if λ approaches zero from above, then the limit motion will take place on the two arcs below and above x -axis. Four periodic trajectories appearing in the limit $\lambda = 0$ correspond to the **A**-atoms in Figure 9. \square

References

- [1] G. Birkhoff, R. Morris, *Confocal conics in space-time*, Am. Math. Monthly **69**(1) (1962), 1–4.
- [2] A. V. Bolsinov, A. T. Fomenko, *Integrable Hamiltonian Systems: Geometry, Topology, Classification*, Chapman and Hall/CRC, Boca Raton, Florida, 2004.
- [3] A. Cayley, *Developments on the porism of the in-and-circumscribed polygon*, Philos. Magazine **7** (1854), 339–345.
- [4] ———, *On the porism of the in-and-circumscribed polygon*, Philos. Trans. Royal Soc. London **51** (1861), 225–239.
- [5] V. Dragović, M. Radnović, *A survey of the analytical description of periodic elliptical billiard trajectories*, J. Math. Sci. **135**(4) (2006), 3244–3255.
- [6] ———, *Integrable billiards and quadrics*, Russian Math. Surveys **65**(2) (2010), 136–197.
- [7] ———, *Poncelet Porisms and Beyond*, Springer, Birkhauser, Basel, 2011.
- [8] ———, *Ellipsoidal billiards in pseudo-Euclidean spaces and relativistic quadrics*, Adv. Math. **231** (2012), 1173–1201.
- [9] D. Genin, B. Khesin, S. Tabachnikov, *Geodesics on an ellipsoid in Minkowski space*, Enseign. Math. **53** (2007) 307–331.
- [10] B. Jovanović, *Noncommutative integrability and action-angle variables in contact geometry*, J. Symplectic Geom. (2012), arXiv:1103.3611.
- [11] B. Khesin, S. Tabachnikov, *Contact complete integrability*, Regul. Chaotic Dyn. **15**(4-5) (2010), 504–520.
- [12] ———, *Pseudo-Riemannian geodesics and billiards*, Adv. Math. **221** (2009), 1364–1396.
- [13] V. Kozlov, D. Treshchëv, *Billiards*, Am. Math. Soc., Providence, RI, 1991,
- [14] R. Ramirez-Ros, *On Cayley conditions for billiards inside ellipsoids*, arXiv:1211.6557, 2012,

Mathematical Institute SANU, Belgrade, Serbia (both authors)
University of Texas, Dallas (V. Dragović)

vladad@mi.sanu.ac.rs
milena@mi.sanu.ac.rs